Mechanisms of Ageing and Development 186 (2020) 111211

Contents lists available at ScienceDirect

Mechanisms of Ageing and Development

journal homepage: www.elsevier.com/locate/mechagedev

Role of sorting nexin PaATG24 in autophagy, aging and development of *Podospora anserina*

Vanessa Henkel, Lea Schürmanns, Miriam Brunner, Andrea Hamann, Heinz D. Osiewacz*

Goethe-University, Institute for Molecular Biosciences, Max-von-Laue-Str. 9, 60438 Frankfurt, Germany

ARTICLE INFO

In memory of Prof. Dr. h.c. mult. Karl Esser (1924–2019) who introduced *P. anserina* as a model system into the field of experimental molecular aging research. He passed away December 3, 2019.

Keywords:
Podospora anserina
Aging
Sorting nexins
Autophagy
Mitophagy
Pexophagy

ABSTRACT

Sorting nexins are a conserved protein family involved in vesicle transport, membrane trafficking and protein sorting. The sorting nexin ATG24/SNX4 has been demonstrated to be involved in different autophagy pathways and in endosomal trafficking. However, its impact on cellular quality control and on aging and development is still elusive. Here we report studies analyzing the function of PaATG24 in the aging model *Podospora anserina*. Ablation of PaATG24 leads to a reduced growth rate, infertility, and to a pronounced lifespan reduction. These characteristics are accompanied by alterations of the morphology and size distribution of vacuoles and severe impairments in non-selective and selective autophagy of peroxisomes (pexophagy) and mitochondria (mitophagy). While general autophagy and pexophagy are almost completely blocked, a PaATG24-independent form of mitophagy is induced during aging. In the *ΔPaAtg24* mutant a strong accumulation of peroxisomes occurs while mitochondrial abundance is only slightly increased. These mitochondria are partially affected in function. Most strikingly, although some PaATG24-independent mitophagy exists, it appears that this is not sufficient to remove dysfunctional mitochondria efficiently enough to prevent premature aging. Overall our data emphasize the key role of mitochondria in aging and of mitophagy in quality control to keep a population of "healthy" mitochondria during aging.

1. Introduction

Maintaining cellular homeostasis by a complex network of quality control pathways is the key for proper development and function of any biological system. Quality control occurs at the level of single molecules, macromolecular complexes, organelles, and whole cells. Impairments in this network lead to dysfunctions, disease and aging (Ahola et al., 2019; Fischer et al., 2012).

We use the filamentous fungus *Podospora anserina* as a model organism to study the molecular basis of organismic aging. In the past, in this system basic pathways and mechanisms have been identified that also in other species, including humans, have an impact on the aging process. For instance, already about 40 years ago, gross rearrangements of the mitochondrial DNA (mtDNA) were first described and subsequently studied in *P. anserina* (Cummings et al., 1979; Kück et al., 1981; Osiewacz and Esser, 1984; Osiewacz et al., 1989; Stahl et al., 1978). Stabilization of the mtDNA was demonstrated to lead to lifespan extension (Hermanns et al., 1994). Subsequently, mtDNA rearrangements and subtle mutations were found to play a key role in aging of other organisms from fungi to humans (Bertrand et al., 1986; Kadenbach et al., 1995; Linnane et al., 1990, 1989; Melov et al., 1995; Piko et al., 1988). Also, age-related alterations in mitochondrial morphology and ultrastructure have been first described in *P. anserina* (Daum et al., 2013; Osiewacz et al., 1989; Scheckhuber and Osiewacz, 2008).

Over the years it has been carefully elaborated that several molecular pathways involved in the control of cellular homeostasis are essential for the characteristic lifespan of *P. anserina*. More recently, we identified autophagy as one of these pathways (Knuppertz et al., 2014; Knuppertz and Osiewacz, 2016). Ablation of PaATG1, a key component of the autophagy machinery, results in a decrease of the wild-type specific lifespan. Moreover, autophagy induction by moderate oxidative stress increases lifespan while excessive stress leads to a lifespan reduction (Knuppertz and Osiewacz, 2017; Knuppertz et al., 2017). The lifespan extending effect of moderate stress, termed mitohormesis (Merry and Ristow, 2016; Ristow and Zarse, 2010), is linked to an increase of selective autophagy of mitochondria (mitophagy) (Knuppertz et al., 2017) acting as a pro-survival quality control pathway by which damaged mitochondria are selectively identified and transported to the vacuole for degradation. In contrast, excessive stress turns autophagy to a pro-death pathway, termed autophagic cell death (ACD), which is distinct from apoptosis, since it is associated with and depends on the formation of autophagosomes and autolysosomes (Kroemer and Levine,

* Corresponding author.
E-mail address: osiewacz@bio.uni-frankfurt.de (H.D. Osiewacz).

https://doi.org/10.1016/j.mad.2020.111211
Received 11 October 2019; Received in revised form 12 December 2019; Accepted 27 January 2020
Available online 30 January 2020

2008). We also demonstrated that autophagy can be modulated by treatment of cultures with natural components like curcumin, a polyphenol from *Curcuma longa* which is long used in traditional medicine. Treatment of *P. anserina* with curcumin was found to lead to an autophagy-dependent lifespan increase (Warnsmann and Osiewacz, 2016). In contrast, treatment with gossypol, a polyphenol from the seeds of cotton plant (*Gossypium spec*) results in the induction of an apoptosis-like type of cell death in *P. anserina* and to autophagic cell death in apoptosis-resistant mammalian glioma cell lines. In both systems the effect of gossypol depends on the mitochondrial permeability transition pore (Kramer et al., 2016; Meyer et al., 2018; Warnsmann et al., 2018). These findings have a potential to experimentally intervene into aging processes and to use natural products for development of therapies against cancer types like gliomas.

Based on these evidences and perspectives we set out to investigate the role of autophagy on aging and development of *P. anserina* in more detail with special emphasis on the impact of different forms of autophagy. We focused on the role of PaATG24 as a putative homolog of ATG24/SNX4 which belongs to the protein family of sorting nexins. These proteins are involved in vesicle transport, membrane trafficking and protein sorting (Haft et al., 1998; Leprince et al., 2003; Nice et al., 2002). They contain an evolutionary conserved PX domain (phox: phagocyte NADPH oxidase) which interacts with phosphoinositides (PIs) enabling an association with endosome membranes (Gallon and Cullen, 2015). According to their domain structure, SNX proteins can be classified into different subfamilies, which either contain the PX-domain only, a PX domain and a FERM domain (protein 4.1/ezrin/radixin/moesin), or a BAR domain (Bin/Amphiphysin/Rvs) acting as a dimerization domain to form dimers with a membrane-binding surface (Chi et al., 2015; Cullen, 2008; Gallon and Cullen, 2015). PaATG24 belongs to the SNX-BAR subfamily. The members of this subfamily preferentially interact with membranes of positive curvature and mediate membrane tubulation and trafficking (Carman and Dominguez, 2018; Cullen, 2008). In yeast, other ascomycetes, and the parasite *Trypanosoma brucei* SNX4 has been shown to be involved in autophagy (Brennand et al., 2015; He et al., 2013; Ma et al., 2017; Nice et al., 2002).

Here we report the role of PaATG24 in aging and development of *P. anserina*. We found that PaATG24 plays a critical role in lifespan control, vegetative growth and sexual reproduction. Deletion of *PaAtg24* leads to alterations in the morphology and size of vacuoles and to a reduction of non-selective and selective autophagy. While the induction of general autophagy and pexophagy appears to be almost completely inhibited, vacuolar degradation of mitochondrial proteins is still possible and increases during aging of the *PaAtg24* deletion mutant. However, this PaATG24-independent mitophagy seems not to be sufficient to counteract the age-related accumulation of dysfunctional mitochondria. Overall our data further emphasize the importance of pathways involved in the control of mitochondrial function and their impact on organism aging.

2. Material and methods

2.1. P. anserina strains and cultivation

The *P. anserina* wild-type strain ‘s’ (Rizet, 1953), previously described reporter strains *PaSod1::Gfp* (Zintel et al., 2010), *PaSod3^{H26L}::Gfp* (Knuppertz et al., 2017), *Gfp::PaAtg8* (Knuppertz et al., 2014) and newly generated *ΔPaAtg24, PaAtg24_Ex3, mCherry-SKL, PaSod3^{H26L}::Gfp-SKL, ΔPaAtg24/PaAtg24_Ex3, ΔPaAtg24/PaSod1::Gfp, ΔPaAtg24/PaSod3^{H26L}::Gfp, ΔPaAtg24/Gfp::PaAtg8, ΔPaAtg24/mCherry-SKL* and *ΔPaAtg24/PaSod3^{H26L}::Gfp-SKL* strains were used in this study. If not otherwise stated, strains were cultivated on standard cornmeal agar (BMM) at 27 °C under constant light conditions (Esser, 1997). Ascospore germination was induced on BMM containing 60 mM ammonium acetate for 2 days at 27 °C in the dark. All strains used in this study were derived from monokaryotic ascospores. For lifespan analysis, determination of the growth rate, fertility assays, for protein preparation, and microscopic analysis, strains were grown on M2 agar plates as previously described by Osiewacz et al. (2013).

2.2. Cloning procedure and generation of P. anserina mutants

All strains were generated in the genetic background of the wild-type strain ‘s’ (Rizet, 1953). Construction of *ΔPaAtg24* was performed as previously described by Hamann et al. (2005). Flanking regions of *PaAtg24* were amplified with oligonucleotides Atg24KO1 (TGCCAACA CCAGCGATACTC Biomers, Ulm, Germany) and Atg24KO2 (GGAAGCT TATGATGGTGGATGGAGGG, HindIII site underlined, Biomers, Ulm, Germany) for 5’-flank and Atg24KO3 (GGACTAGTGCCGACTGAGTTG GTTTG, BcuI site underlined, Biomers, Ulm, Germany) and Atg24KO4 (AAGCGGCCGCGAATTGTGTCTCTTTGAG, NotI site underlined, Biomers, Ulm, Germany) for 3’-flanking region. The fragments were cloned in the plasmid pKO4 (Hamann et al., 2005; Luce and Osiewacz, 2009) digested with SmaI, HindIII, BcuI and NotI (Thermo Scientific ER0661, ER0501, ER1251, ER0591). With a *PaAtg24*-containing cosmid of a representative cosmid library (Osiewacz, 1994), the resulting plasmid pAtg24KO2 was used for generation of a *ΔPaAtg24* cosmid, as described before (Hamann et al., 2005). This cosmid contains a phleomycin resistance cassette with more than 3 kbp *PaAtg24* flanking regions for directed gene replacement. Subsequently, transformation was performed into *P. anserina* wild-type spheroplasts as described before (Osiewacz et al., 1991). Selection of transformants was performed by growth on phleomycin (Genaxxon, M3429) containing medium. For complementation analysis, *PaAtg24* was amplified with Atg24-2 (ATA GATCTCCAGTTCTGGCAGCAGAG, BglII underlined, Biomers, Ulm, Germany) and Atg24-5 (CGGGTCTAGATGAGCAGCATGTTATTGG, XbaI underlined, Biomers, Ulm, Germany) and cloned into the plasmid pKO7 (Kunstmann and Osiewacz, 2009) digested with BglII (Thermo Scientific, ER0081) and XbaI (Thermo Scientific, ER0681) containing a hygromycin B resistance cassette. After transformation of the resulting pAtg24Ex3 plasmid in *ΔPaAtg24* spheroplasts as previously described (Osiewacz et al., 1991) selection was performed on hygromycin B (Calbiochem, 400051) containing medium. To construct the pexophagy reporter strain *PaSod3^{H26L}::Gfp-SKL,* the *PaSod3^{H26L}::Gfp* fusion gene (without mitochondrial targeting sequence) was amplified with oligonucleotides Sod3-LS-1 (CTCGGATCCATGAAGGCCACTCTC, BamHI underlined, Biomers, Ulm, Germany) and GFP-2 (GGTCTAGATTAGAGCT TGCTCTTGTACAGCTCGTCCATGC, XbaI underlined, Biomers, Ulm, Germany). The fragment was cloned into the plasmid pExMtterhph (Luce and Osiewacz, 2009), digested with BamHI and XbaI (Thermo Scientific, ER0051, ER0681). The final plasmid pSod3^{H26L}Gfp-SKL was transformed into *P. anserina* wild-type spheroplasts as previously described (Osiewacz et al., 1991).

For the peroxisome reporter strain *mCherry-SKL,* the *mCherry* gene was amplified from the plasmid pmCherry (Clontech, 632522) with oligonucleotides GFP-1 (CGCGGATCCATGGTGAGCAAGGGCGAG, BamHI underlined, Biomers, Ulm, Germany) and GFP-2 (GGTCTAGAT TAGAGCTTGCTCTTGTACAGCTCGTCCATGC, XbaI underlined, Biomers, Ulm, Germany). The fragment was digested with BamHI and XbaI (Thermo Scientific, ER0051, ER0681) and was cloned in the plasmid pExMtterhph (digested with BamHI and XbaI, (Luce and Osiewacz, 2009). The plasmid pmCherry-SKL was transformed into *P. anserina* wild-type spheroplasts as described by Osiewacz et al. (1991).

Double mutants were generated after crossing two mutant strains followed by selection of strains from the progeny containing both mutations.

2.3. Fertility analysis and determination of spermatia number

Fertility analysis was performed by spermatization experiments. In these experiments mycelia of the respective monokaryotic strains were

cultivated on M2 agar under constant light at 27 °C. Spermatia were harvested by flooding the plate with 5 ml sterile H_2O for 5 min. Droplets of 300 µl of this suspension, which contained spermatia of the corresponding strain, were pipetted onto a strain serving as the female partner. The spermatia suspension was carefully removed after 5 min of incubation. After cultivation of the mycelium for 5 days, the number of perithecia was determined. The number of perithecia obtained from crosses of the wild type with another wild-type partner was set to 100 %. For measurement of spermatia numbers the respective mycelium was cultivated for 9 days on M2 agar plates. After flooding the mycelium with 2 ml sterile H_2O for 5 min, the suspension was centrifuged for 10 min at 18,400 *g*, RT. The pellet was resuspended in 200 µl TPS buffer (Osiewacz et al., 2013) and spermatia counted in a Thoma chamber.

2.4. Growth rate and lifespan determination

Lifespan and growth rate analysis on M2 medium with monokaryotic ascospores was performed according to Osiewacz et al. (2013). For analysis of peroxisomal and mitochondrial functionality M2 medium was used, in which dextrin was replaced by 0.2 % Tween® 40 (Sigma-Aldrich, P1504) and 0.05 % oleic acid (Sigma-Aldrich, O1008) or 0.01 % glycerol (Roth, 4043.3).

2.5. Western blot analysis

For extraction of total protein extracts, mycelia from different *P. anserina* strains were cultivated on M2 medium covered with cellophane foil for 2 days at 27 °C under constant light followed by cultivation in CM liquid medium (Osiewacz et al., 2013) for 3 days at 27 °C under constant light and shaking. After harvesting the mycelia via filtering, 250 mg mycelium was transferred into a tube filled with glass beads (Precellys Lysing Kit, Bertin Technologies, KT0393-1-004.2) and mixed with 2 volumes protein extraction buffer (Osiewacz et al., 2013) or, in case of pexophagy analysis, with 3 volumes TUS buffer (62.5 mM TRIS-HCl pH 8, 4 M urea, 3 % SDS, 100 mM DTT). Homogenization was performed with 2 × 25 s, 5800 rpm and 10 s resting in a homogenizer (Precellys 24-Dual Homogenisator, Bertin Technologies). After centrifugation for 5 min at 9300 *g*, 4 °C, supernatant containing total protein extract was used for western blot analysis. After fractionation of proteins by 2-phase SDS-PAGE (12 % separating gels) according to standard protocols (Brust et al., 2010), proteins were transferred to PVDF membranes (Immobilon-FL PVDF, Millipore, IPFL00010). Blocking, antibody incubation and washing steps were performed according to the Odyssey® Imaging System Western blot analysis protocol (LI-COR Biosciences, Bad Homburg, Germany). Primary antibody anti-GFP (mouse, 1:10,000 dilution, Sigma-Aldrich, G6795) and anti-PaATG24 (rabbit, 1:10,000 dilution, peptide antibody raised against RGVDHEQARRDRLRKLELR, Davids Biotechnologie GmbH, Regensburg, Germany) were used. IRDye® 680RD goat anti-mouse (1:15,000 dilution, LI-COR Biosciences, 926–68070) and IRDye® 680 LT goat anti-rabbit (1:20,000 dilution, LI-COR Biosciences, 926–68021) served as secondary antibodies. The Odyssey® infrared scanner (LI-COR Biosciences, Bad Homburg, Germany) system was used for detection and quantification was done with the manufacturer's software (Odyssey® Infrared Imaging System – Application Software Version 3.0).

2.6. Southern blot analysis

DNA isolation of *P. anserina* was carried out as described before (Lecellier and Silar, 1994). Digestion of DNA, gel electrophoresis and Southern blotting was performed in accordance with standard protocols. Southern blot hybridization and detection was carried out as described in manufacturer's protocol with digoxigenin-labeled hybridization probes (DIG DNA Labeling Mix, Sigma-Aldrich, 11175033910). The *PaAtg24*-, *hygromycin*- and *phleomycin*-specific probes were generated from plasmids containing the respective genes via restriction with suitable enzymes. As *PaAtg24* probe the 685 bp NcoI/XhoI-fragment was used, for the hygromycin resistance cassette (*hph*) the 737 bp BcuI/NcoI-fragment and for the phleomycin resistance cassette (*Ble*) a 1293 bp BamHI-fragment was used as hybridization probe, each containing a part of the respective gene.

2.7. Fluorescence microscopy

For microscopic analysis, *P. anserina* strains were cultivated on glass slides with a central depression containing M2 medium or M2-N medium (M2 lacking the nitrogen source urea) for 1 day at 27 °C under constant light. Microscopic analysis was performed with Zeiss Cell Observer SD – Spinning Disk Confocal Microscope (Carl Zeiss Microscopy, Jena, Germany) with a 63x/1.4 oil objective lens (Carl Zeiss Microscopy, Jena, Germany).

For autophagosome quantification, representative z-stack images of *ΔPaAtg24/Gfp::PaAtg8* and *Gfp::PaAtg8* strains at respective ages were acquired. ZEN 2.3 SP1 (black) was used for the generation of maximum intensity projection images and ImageJ 1.520 for analysis. Threshold for hyphal background was determined by MaxEntropy setting, threshold for autophagosomes was set manually and autophagosome number were counted via the "analyze particles" setting. The size of measured autophagosomes was limited to 0.2–1.5 µm to prevent counting vacuoles already containing GFP::PaATG8 instead of autophagosomes. For analysis of vacuoles, respective strains were treated for 5 h with 2 µg/ml FM™ 4–64 Dye (Invitrogen, T13320) before microscopic analysis. The size and distribution of vacuoles was manually measured using ZEN 2.5 (blue).

2.8. Phylogenetic and cluster analysis

Clustal analysis and generation of phylogenetic tree was performed with Clustal Omega Multiple Sequence Alignment (https://www.ebi.ac.uk/Tools/msa/).

2.9. Statistical analysis

For statistical analyses, the paired Student *t*-test was used to compare the respective samples with the appropriate wild-type samples. The threshold for statistical significance was at $p > 0.05$ not significant, significant ($p < 0.05$): *; highly significant ($p < 0.01$): **; very highly significant ($p < 0.001$): ***. All data shown are the mean ± standard error of the median (SEM).

3. Results

3.1. PaATG24 is homolog to ATG24/SNX4 proteins from other organisms

In a previous study MoATG24 was identified to play a role in the control of mitophagy and development of the filamentous fungus *Magnaporthe oryzae* (He et al., 2013). In order to unravel the role of a potential *P. anserina* homolog in aging and development, we performed a protein BLAST search and identified PODANS_1_1920 (Uniprot B2A9V5) as such a protein. It shares 62.9, 32.5, and 25.6 % amino acid identity with the corresponding sorting nexins of *M. oryzae, Saccharomyces cerevisiae*, and *Homo sapiens,* respectively, and displays the typical domain architecture of ATG24/SNX4 proteins (Supplement Fig. 1 A). Phylogenetic analysis revealed, that ATG24 sorting nexins are evolutionary conserved among species (Supplement Fig. 1 B).

3.2. PaATG24 is required for normal vegetative growth, lifespan, and sexual development

In order to unravel the function of PaATG24 in *P. anserina*, we isolated a cosmid from a representative cosmid library of the wild type (Osiewacz, 1994) which contains the *PaAtg24* reading frame and 5' and

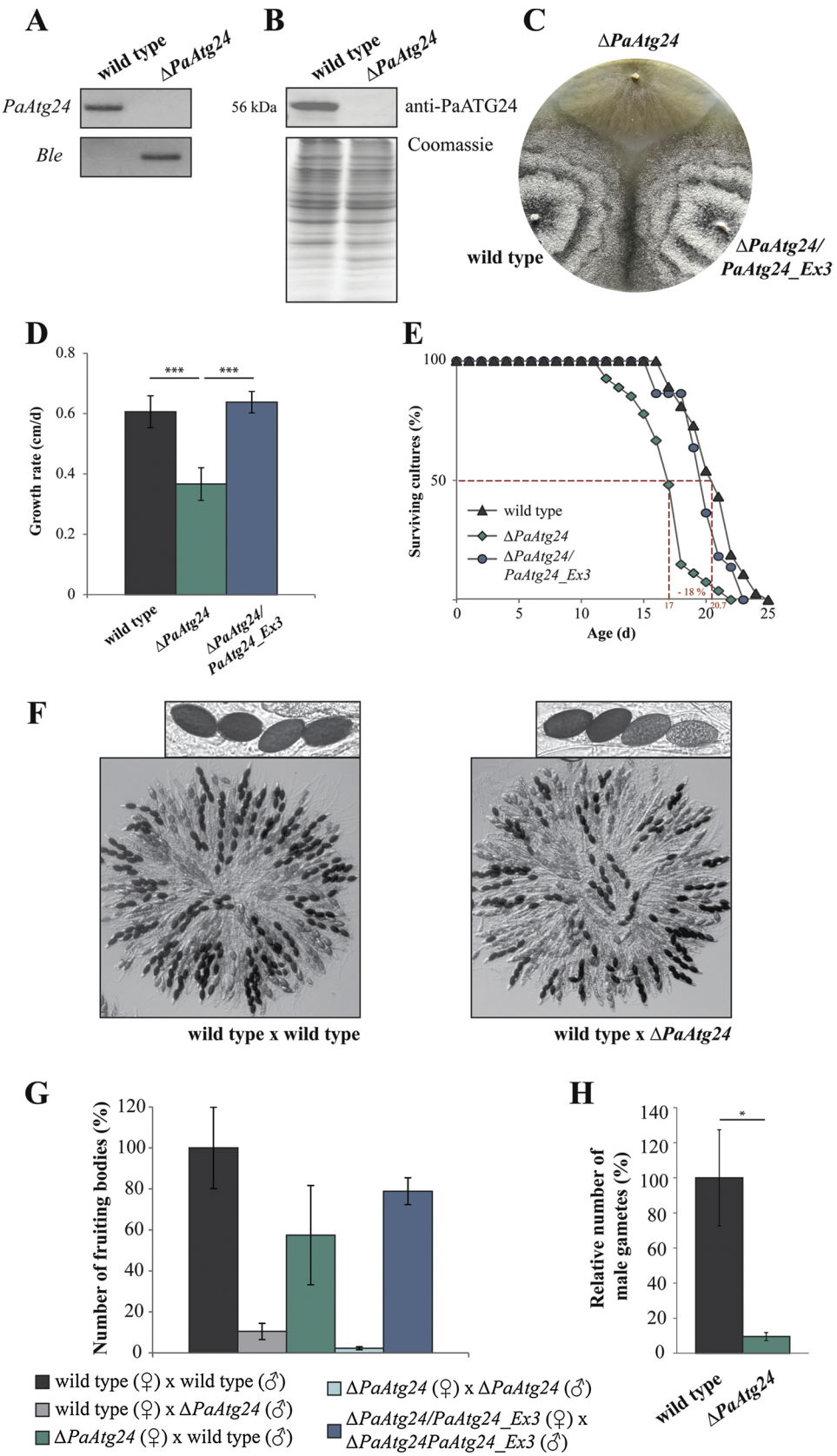

Fig. 1. Deletion of *PaAtg24* leads to hypopigmentation, shortened lifespan, reduced growth rate and male sterility.
(A) Southern blot analysis verifies the replacement of *PaAtg24* by a phleomycin resistance gene (*Ble*). (B) Western Blot analysis of total protein extracts of *ΔPaAtg24* and wild type with anti-PaATG24 antibody. The coomassie-stained gel serves as loading control. (C) Phenotypes of *ΔPaAtg24,* complementation strain *ΔPaAtg24/PaAtg24_Ex3*, and the wild type at the age of 10 days. Strains were grown on M2 medium at 27 °C and constant light. (D, E) Growth rate and lifespan of *ΔPaAtg24* (n = 25) in comparison to wild type (n = 23) and complementation strain *ΔPaAtg24/PaAtg24_Ex3* (n = 23). The dashed line represents the median life span of the strains. (F) Comparison of asci from fruiting bodies of crossing two wild-type strains and of a cross of *ΔPaAtg24* with the wild type. (G) Number of fruiting bodies on mycelia resulting from the spermatization of the wild type and *ΔPaAtg24* (n = 3, each) with male (♂) or female (♀) partner, respectively. The complementation of the impairment in fertility of *ΔPaAtg24* was tested by spermatization of *ΔPaAtg24* strain expressing a wild-type *PaAtg24* gene. (H) Number of male gametes of wild type and *ΔPaAtg24* (n = 6, each), pointing out the impaired formation of male gametes (spermatia) in the mutant. Samples were statistically analyzed with two-tailed *t*-test (* = $p \leq 0.05$, ** = $p \leq 0.01$, and *** = $p \leq 0.001$).

3' flanking sequences of sufficient length for gene replacement by a two-step strategy (Hamann et al., 2005). Southern and western blot analysis verified the absence of *PaAtg24* sequences and of the PaATG24 protein in the selected deletion strain *ΔPaAtg24* (Fig. 1 A, B).

The subsequent characterization of this strain revealed pleiotropic effects. In comparison to the wild type, the mutant displays a reduced formation of aerial hyphae and a decreased pigmentation of the vegetation body. In addition, the growth rate and the lifespan are reduced.

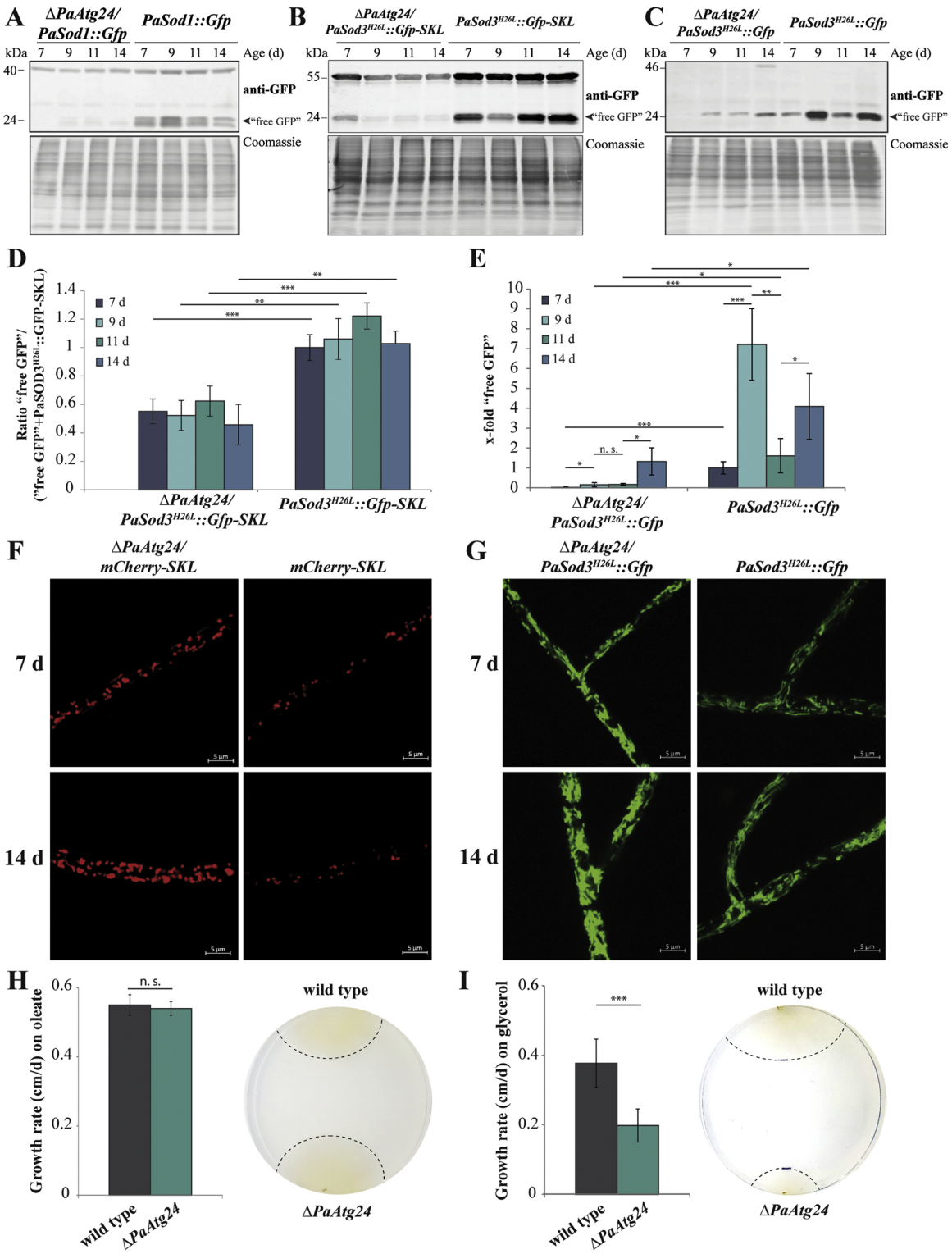

Fig. 2. PaATG24 is required for non-selective and selective autophagy of peroxisomes and mitochondria.
(A–C) Western blot analysis of cytosolic reporter protein PaSOD1::GFP, peroxisomal localized reporter protein PaSOD3^{H26L}::GFP-SKL and mitochondrial reporter protein PaSOD3^{H26L}::GFP with a GFP-tagged inactive form of a mitochondrial superoxide dismutase in 7-, 9-, 11- and 14-day-old *ΔPaAtg24* and control strains (n = 4, each) with an antibody against GFP. Ablation of "free GFP" in *ΔPaAtg24* demonstrates an impaired non-selective autophagy, pexophagy or mitophagy in the mutant. (D) Quantification of pexophagy by western blot analysis in 7-, 9-, 11- and 14-day-old *ΔPaAtg24/PaSod3^{H26L}::Gfp-SKL* and *PaSod3^{H26L}::Gfp-SKL* strains (n = 4, each) after normalization to the coomassie-stained gel and determination of the ratio of "free GFP" to "free GFP" and fusion protein. (E) Quantification of "free GFP" of *ΔPaAtg24/PaSod3^{H26L}::Gfp* and *PaSod3^{H26L}::Gfp* at different age stages (n = 4, each) by western blot analysis with an anti-GFP antibody for analysis of mitophagy. The samples were normalized to the coomassie-stained gel and protein levels of 7-day-old wild type were set to 1. (F, G) Microscopic analysis of peroxisomes and mitochondria in *ΔPaAtg24* and control strains with peroxisomal reporter mCHERRY-SKL and mitochondrial reporter PaSOD3^{H26L}::GFP in 7- and 14-day-old strains. While peroxisome number increases during aging of the deletion mutant and compared to the control strain, mitochondria are only slightly increased in 7-day-old *ΔPaAtg24*. During aging no significant accumulation of mitochondria is observed. (H, I) The growth rate of *ΔPaAtg24* on M2 medium with oleate restores the reduced growth rate of *ΔPaAtg24* in comparison to wild type on standard M2 medium. In contrast to the wild type, the growth rate of *ΔPaAtg24* on M2 medium with glycerol is strongly decreased. For statistical analysis, the two-tailed *t*-test was used (* = $p \leq 0.05$, ** = $p \leq 0.01$, and *** = $p \leq 0.001$).

These phenotypic changes are restored to wild-type characteristics via the reintroduction of the wild-type copy of *PaAtg24* into *ΔPaAtg24* (Fig. 1 C–E).

In *P. anserina* sexual propagation is controlled by the two mating type loci *mat-* and *mat+*. In nature, reproduction of *P. anserina*, which does not produce vegetative propagation units like conidia, proceeds via meiospores. In the vast majority, these ascospores contain two haploid nuclei with opposite mating types in one spore. The vegetation bodies (mycelia) developing from these ascospores are therefore also heterokaryotic and produce male gametes (spermatia) and female gametangia (protoperithecia) of both mating types. As a consequence, such cultures are self-fertile and form fruiting bodies and ascospores without the need to contact another partner. In very rare cases, monokaryotic cultures arise from small ascospores that are generated due to impairments in spore formation. These cultures produce spermatia and protoperithecia of only one mating type. For sexual reproduction they need to contact a partner of the opposite mating type. While these monokaryotic ascospores basically do not play a role in natural reproduction, they allow the experimental analysis of sexual development in some detail (Osiewacz, 1996; Osiewacz et al., 2013).

Such an analysis revealed that heterokaryotic *ΔPaAtg24* strains do not produce fruiting bodies and are completely sterile. This is also the case in confrontational crosses in which two monokaryotic *ΔPaAtg24* strains of the opposite mating type are grown on the same agar plate, contact each other, exchange genetic material and initiate sexual reproduction. A confrontational cross between *ΔPaAtg24* and the wild type leads to fruiting body formation. Significantly, dikaryotic ascospores containing two *ΔPaAtg24* nuclei display a reduced pigmentation and a developmental delay in maturation (Fig. 1 F, right).

Similar results are obtained in spermatization experiments (Osiewacz, 1996) in which collected spermatia of monokaryotic *ΔPaAtg24* strains of one mating type are poured on monokaryotic *ΔPaAtg24* cultures of the opposite mating type. In this case, no or only very few fruiting bodies are formed (Fig. 1 G). In accordance, compared to wild-type cultures fertilized by wild-type spermatia, spermatization of wild-type cultures by spermatia of the *ΔPaAtg24* strain leads to a 90 % reduction of fruiting body number. A reduction of fruiting bodies to about 40 % is observed when *ΔPaAtg24* cultures are fertilized by spermatia of the wild type (Fig. 1 G). These data demonstrate that, while the formation of both female gametangia and male gametes of the *PaAtg24* deletion strain are impaired, male fertility is most severely affected. The determination of the number of spermatia explains this strong effect as the result of a strong reduction of 90 % in spermatia formation (Fig. 1 H).

3.3. PaATG24 is required for non-selective autophagy and selective autophagy

Next we set out to investigate the molecular role of PaATG24 on *P. anserina* aging and development. Since ATG24 proteins of other fungi are known to impact mitophagy and pexophagy and most likely also general autophagy (Ano et al., 2005; He et al., 2013; Ma et al., 2018), we focused on the analysis of these types of autophagy. First, we used a protein degradation assay that was previously established for *P. anserina* (Knuppertz et al., 2014). This assay monitors the vacuolar degradation of marker proteins, and thus of autophagy, via the detection of the degradation resistant GFP-part ("free GFP") of a marker fusion protein. Analysis of strains expressing these specific GFP-fusion genes allows the discrimination between non-selective and selective autophagy. For such an analysis, we first generated strains expressing the genes coding for the specific marker proteins in the *ΔPaAtg24* genetic background. We selected the corresponding double mutants for the analysis of non-selective autophagy and mitophagy from crosses of the *ΔPaAtg24* mutant with strains expressing the cytosolic *PaSod1::Gfp* marker gene or *PaSod3^{H26L}::Gfp* which codes for a modified mitochondrial marker protein with a mitochondrial targeting sequence (Knuppertz et al., 2017). For the analysis of pexophagy we had first to generate a *P. anserina* strain that produces a newly constructed pexophagy GFP-marker protein. This protein consists of the inactive superoxide dismutase PaSOD3 (PaSOD3^{H26L}) fused to GFP. In this construct the mitochondrial targeting sequence of PaSOD3 was removed and the peroxisomal SKL targeting signal of *P. anserina* (Ruprich-Robert et al., 2002) was added at the C-terminus. The resulting strain, *PaSod3^{H26L}::Gfp-SKL*, was subsequently crossed with *mCherry-SKL* to analyze if PaSOD3^{H26L}::GFP-SKL localizes to peroxisomes. A fluorescence microscopic analysis (data not shown) revealed that PaSOD3^{H26L}::GFP-SKL and mCHERRY-SKL colocalize verifying the peroxisomal localization of PaSOD3^{H26L}::GFP-SKL. Subsequently the strain was crossed with *ΔPaAtg24* and the resulting *ΔPaAtg24/PaSod3^{H26L}::Gfp-SKL* double mutant was selected and verified by Southern blot analysis (Supplement Fig. 2A).

Next we investigated the impact of PaATG24 on general autophagy, pexophagy and mitophagy. We compared the vacuolar degradation of the cytoplasmic, peroxisome- and mitochondria-specific marker proteins in strains of different age, which express *PaAtg24* with those in which this gene is deleted (Fig. 2 A–C). We found that, compared to strains containing a functional *PaAtg24* gene, in the *ΔPaAtg24* strains expressing the cytoplasmic and peroxisomal marker genes almost no "free GFP" was observed. These results demonstrate that PaATG24 strongly impacts general autophagy and pexophagy (Fig. 2 A, B). Moreover, no significant age-dependent differences in pexophagy was found after analysis of the ratio of "free GFP" to "free GFP" and the fusion protein (Fig. 2 B, D). In clear contrast and most strikingly, in strains expressing the gene for the mitochondrial marker protein, low amounts of "free GFP" were observed in young cultures (Fig. 2 C, E). During aging "free GFP" increases but does not reach the levels of *PaAtg24* expressing strains of the same chronological age (Fig. 2 C, E).

The increase of "free GFP" between 9- and 11-day old control strains which is also visible with the PaSOD1::GFP reporter is likely due to specific requirements during the life cycle of *P. anserina* (Knuppertz and Osiewacz, 2016). After about one week of growth *P. anserina* mycelia form female reproduction structures, a process for which autophagy appears to be required, most probably to ensure sufficient nutrient supply (Pinan-Lucarré et al., 2003). The lack of detectable amounts of the fusion protein PaSOD3^{H26L}::GFP results from very low abundance in total protein extracts. In mitochondrial preparations, the fusion protein is clearly visible (Knuppertz et al., 2017). However, even without data on the amount of the fusion protein, the level of "free GFP" is a measure of mitophagic flux, since this degradation product only occurs upon vacuolar degradation of the fusion protein. The observation of clearly visible "free GFP" in the mutant indicates the presence of a PaATG24-independent form of mitophagy that appears not to exist for general autophagy and pexophagy. It may be a form of micromitophagy in which parts of mitochondria, so-called mitochondria-derived vesicles (MDVs), are formed which contain damaged mitochondrial proteins. These vesicles bud off from mitochondria and fuse with the vacuole/lysosome (Lemasters, 2014).

In order to analyze the consequences of the PaATG24 ablation on peroxisomes and mitochondria we performed a laser scanning microscopy analysis of strains expressing organelle specific marker genes (Fig. 2 F, G). For analysis of peroxisomes, we used a newly constructed strain producing mCHERRY-SKL. The analysis of mitochondria was performed with strains expressing *PaSod3^{H26L}::Gfp*, encoding a modified mitochondrial superoxide dismutase isoform of *P. anserina* (Knuppertz et al., 2017). The two marker genes were either expressed in the wild-type or in the *PaAtg24* deletion background.

We found that, compared to the strain expressing *PaAtg24*, peroxisome abundance is strongly increased in the PaATG24-ablated strain of 7- and 14-days of age (Fig. 2 F). In contrast, only a slight increase of mitochondrial abundance is found in PaATG24-containing and PaATG24-ablated strains of both 7- and 14-days of age (Fig. 2 G). These results were confirmed by western blot analysis of two mitochondrial

proteins (Supplement Fig. 2 B–D).

Next we analyzed the functional status of peroxisomes and mitochondria in *ΔPaAtg24* strains by growing them on media containing oleate or glycerol as sole carbon source (Fig. 2 H, I). These carbon sources are metabolized by peroxisomes or mitochondria, respectively. We found the growth rate of *ΔPaAtg24* on oleate was comparable to that of the wild type indicating that the increased number of peroxisomes in the mutant corrects potential metabolic impairments in *ΔPaAtg24* (Fig. 2 H). In striking contrast, on glycerol medium the growth rate of the mutant was almost 50 % slower than that of the wild type (Fig. 2 I). Thus, although some mitophagic flux occurs in the mutant that increases during aging, a larger fraction of mitochondria of the *ΔPaAtg24* appears to be dysfunctional. Full mitophagy capacity, as it occurs in the wild type, seems to be a very effective pathway in keeping a "healthy" population of mitochondria during aging.

3.4. Ablation of PaATG24 leads to decreased vacuolar degradation and is linked to changes in the morphology and size of vacuoles

In a next series of experiments we set out to determine whether or not PaATG24 is involved in the control of macroautophagy which requires the formation of autophagosomes and their fusion with vacuoles. First, we analyzed autophagosome numbers in 7- and 14-day-old strains expressing *Gfp::PaAtg8* as an autophagosomal marker gene (Knuppertz et al., 2014) in the wild-type and the *PaAtg24* deletion background (Fig. 3 A, B). To discriminate between GFP::ATG8 puncta and vacuolar structures a co-staining with FM4–64, a dye which localizes to vacuolar membranes, was performed (Supplement Fig. 2 E). Since there was no colocalization of GFP and FM4–64 signals, GFP::PaATG8 puncta represent autophagosomes. Quantification of these puncta revealed a three times higher number of autophagosomes in the absence of PaATG24 in 7-day-old strains (Fig. 3 B). In the old *ΔPaAtg24* strain (14 days) autophagosomes appear to be larger and the number is two times higher than in the control strain of the corresponding age. Defective fusion of autophagosomes with the vacuole may lead to the observed accumulation. To verify this possibility we performed a western blot analysis with GFP::PaATG8 as reporter (Fig. 3 C, D). Quantification of "free GFP" normalized to the GFP::PaATG8 fusion protein revealed that in the strain containing PaATG24 vacuolar degradation remains stable at the two analyzed ages (Fig. 3 D). In contrast, GFP::PaATG8 degradation is slightly, but significantly decreased in 7-day-old *ΔPaAtg24*. In 14-day-old *ΔPaAtg24* cultures a profound decrease by about 50 % is observed. We conclude that PaATG24 is involved in autophagic flux.

In order to analyze this process in some more detail, we next investigated the impact of PaATG24 on vacuole function. First, we analyzed the size of vacuoles in the *PaAtg24* expressing strain and the *PaAtg24* deletion strain in 7- and 14-day-old cultures (Fig. 4 A–C). Vacuole formation was induced by nitrogen starvation of the wild type and *ΔPaAtg24* for one day. Subsequently, vacuolar membranes were stained with FM4–64 followed by the determination of vacuolar size. We categorized the organelles into small vacuoles with an area of less than 2.5 μm^2, medium-sized vacuoles of 2.5–8 μm^2, and vacuoles larger than 8 μm^2. In 7-day-old wild-type cultures vacuoles displayed an oval morphology and cover 30 % of the hyphal area (Fig. 4 A, B). We found that 50 % of these vacuoles are of small, 45 % of medium, and 5 % of large size (Fig. 4 C). Compared to 7-day-old wild-type cultures, hyphal area covered by vacuoles of 14-day-old cultures was increased to up to 38 % (Fig. 4 B). Vacuole size distribution was changed in the older cultures to 64 % small, 34 % medium, and 2 % large sized vacuoles (Fig. 4 C).

Vacuoles of the *PaAtg24* deletion strain are smaller than those of the wild type, are round and cover a smaller hyphal area than vacuoles of the *PaAtg24* expressing strain (Fig. 4 A, B). In 7-day-old *ΔPaAtg24* the vacuole-covered area is 25 % and 29 % in 14-day-old cultures. Beside this impact on vacuolar shape, we found that in 7-day-old strains 78 % of the mutant vacuoles are smaller than 2.5 μm^2, 22 % are middle-sized and no vacuoles are found in the large category (Fig. 4 C). In comparison, in 14-day-old cultures vacuole size increases and 40 % display a medium size. Again, no large-sized vacuoles are found (Fig. 4 C).

Finally, we investigated whether autophagosome-vacuole fusion is affected in PaATG24 ablated strains. To this end, vacuole formation and autophagy was induced in 7- and 14-day-old strains expressing *Gfp::PaAtg8* by nitrogen starvation for one day. Subsequent confocal laser scanning microscopy analysis revealed that in both, the *PaAtg24* expressing as well the *PaAtg24* deletion strain, GFP localizes to the vacuole (Fig. 4 D, Supplement Fig. 3 A) demonstrating that fusion of autophagosomes with the vacuole is possible in the mutant. Quantification of the intensity of vacuolar GFP in comparison to total hyphal GFP revealed a slight, but not significant lower amount of GFP in the small *ΔPaAtg24* vacuoles in comparison to the wild-type control (Supplement Fig. 3 B). These rather minor impairments in fusion of autophagosomes with the vacuole can thus not explain the strongly reduced autophagic flux in *ΔPaAtg24*.

We conclude that the observed impairments in autophagy of the *PaAtg24* deletion strain are due to the reduced vacuole size and cell volume coverage by vacuoles lowering the capacity of autophagic/vacuolar degradation.

4. Discussion

In order to more specifically analyze the impact of autophagy on mitochondria and aging in *P. anserina*, we started to investigate the role of mitophagy in more detail. At that time it was reported that the sorting nexin ATG24 localizes to mitochondria and that it is involved in mitophagy and asexual development of the fungal rice pathogen *M. oryzae*. Moreover, the reduced production of vegetative spores (conidia) in the *MoAtg24* deletion strain was increased via the expression of *ScAtg32* encoding a yeast mitophagy cargo receptor (He et al., 2013). Because of this strong link of ATG24 to mitophagy we set out to investigate its role in aging and development of *P. anserina*.

Most strikingly, in contrast to what has been suggested by He et al. (2013) for *M. oryzae,* both general autophagy as well as pexophagy is severely affected in the *PaAtg24* deletion strain of *P. anserina*. In the yeasts *S. cerevisiae*, *Schizosaccharomyces pombe* and *Pichia pastoris* an impact of ATG24 orthologs on selective autophagy has been described (Ano et al., 2005; Nice et al., 2002; Zhao et al., 2016). In addition, ScSNX4 has been shown to coordinate autophagic degradation of proteasomes and ablation of this sorting nexin results in a cytoplasmic aggregation of proteasomes (Nemec et al., 2017). Only in *S. cerevisiae* some evidence about a role in the control of non-selective autophagy exists because a double mutant, in which the genes coding for ScSNX4 (ScATG24) and the phosphatidylserine decarboxylase 1 (ScPSD1) are deleted, was found to be defective in autophagy under starvation conditions (Ma et al., 2018).

The deletion of *PaAtg24* was found to display a severe pleiotropic effect. Most strikingly, we observed that colonies arising from a single heterokaryotic ascospore are completely sterile and are not able to form fruiting bodies. The involvement of autophagy in *P. anserina* development was shown before in *ΔPaAtg1* and *ΔPaAtg8* mutants, which display an impaired spore formation and delayed spore germination (Knuppertz et al., 2014; Pinan-Lucarré et al., 2005). Also in *Aspergillus nidulans AnAtg8* deletion impairs fertility (Kikuma et al., 2006). In contrast to many other fertility mutants of *P. anserina* in which the female sexual reproduction units are severely impaired, in *ΔPaAtg24* it is the formation of functional male gametes that is most severely affected. Some clues towards the understanding of underlying mechanisms come from a recent study (Takano-Rojas et al., 2016). In this study it was found that 91 % of the investigated wild-type microconidia (spermatia) do contain only 1–6 peroxisomes, while 9 % had no peroxisomes at all. In addition, it was shown that the number of peroxisomes at later stages of sexual development is strongly down-regulated implying the

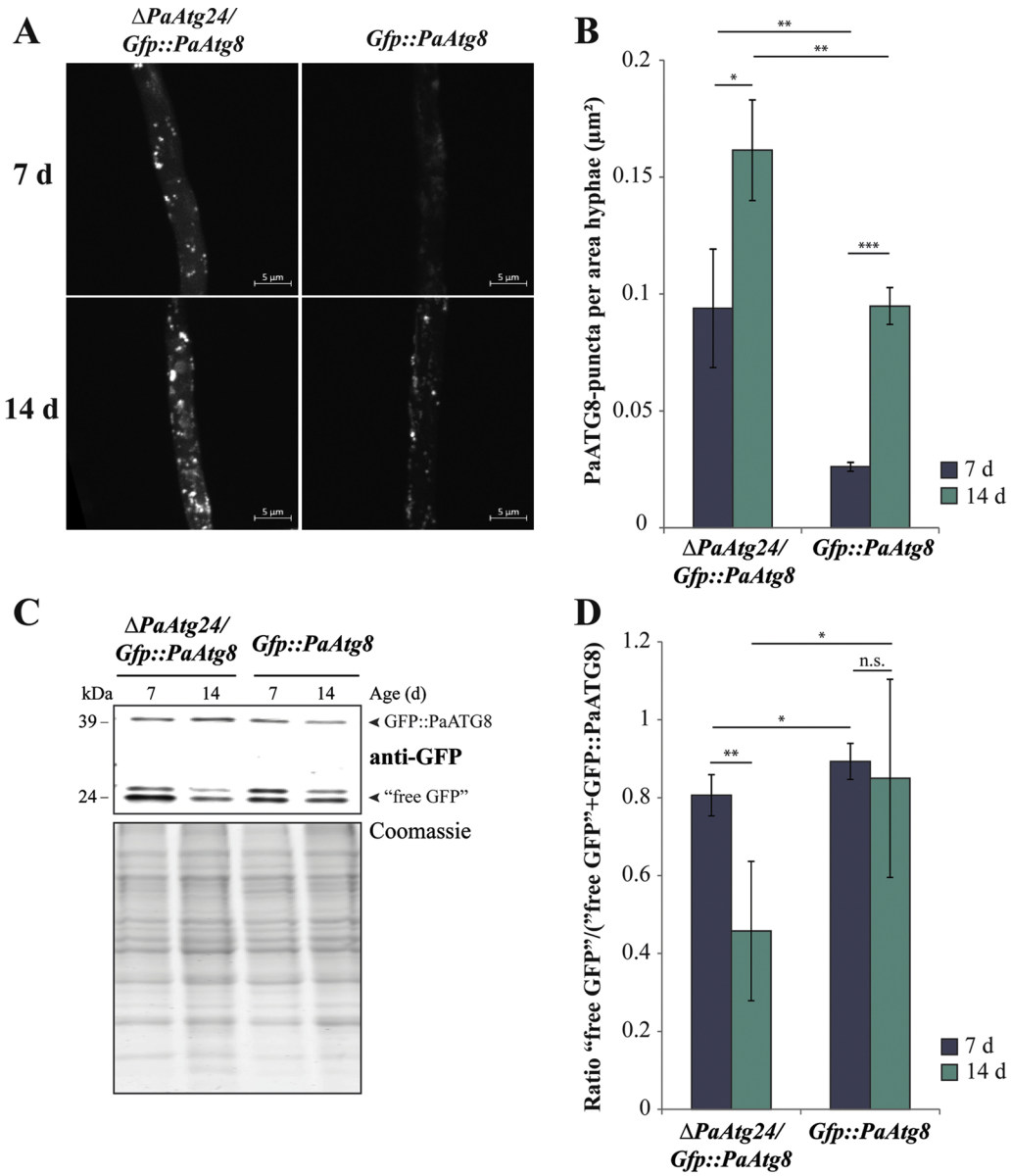

Fig. 3. Ablation of PaATG24 leads to an increased autophagosome number and reduced autophagosomal flux.
(A, B) Fluorescence microscopy and quantification of autophagosomes in 7- and 14-day-old *ΔPaAtg24/Gfp::PaAtg8* and *Gfp::PaAtg8* strains (n = 3, each) after cultivation on M2 medium indicates an increased amount of autophagosomes in *ΔPaAtg24* in both age stages. (C, D) Western blot analysis of total protein extracts of 7- and 14-day-old *ΔPaAtg24/Gfp::PaAtg8* and *Gfp::PaAtg8* as control (n = 4, each) and quantification of ratio "free GFP" to "free GFP" + fusion protein displaying a reduced autophagosome degradation in the mutant strain. Normalization of the samples was done with the coomassie-stained gel. All samples were statistically analyzed with two-tailed *t*-test (* = $p \leq 0.05$, ** = $p \leq 0.01$, and *** = $p \leq 0.001$).

involvement of pexophagy. The observed impact on pexophagy and the strong increase of peroxisomes in mycelia of *ΔPaAtg24* may explain the strongly reduced formation of spermatia in the mutant. In contrast to this effect on sexual reproduction in *P. anserina*, it is vegetative propagation that is affected in the ascomycetes *M. oryzae* and *Fusarium graminearum*. In these species, which efficiently reproduce by vegetative spores (conidia), the formation of conidia is strongly reduced in the corresponding ATG24 ablation mutants (He et al., 2013; Lv et al., 2017). Overall the existing data emphasize a key role of autophagy in fungal development. Additionally, the pronounced reduction in male gamete number in *ΔPaAtg24* may result from impairments in fusion and septation processes which are needed during the formation of male gametes. These cells are formed via septation of parts of the multi-nucleate, coenocytic filamentous cells of the vegetation body. Such a role of ATG24/SNX4 in septation processes might also explain the conidiation defect observed in *M. oryzae* and *F. graminearum* (He et al., 2013; Lv et al., 2017) since conidia formation also requires septation.

In addition to the profound effects on sexual reproduction, the deletion of *PaAtg24* impacts the aging process and, compared to the wild type, leads to a decreased lifespan. Surprisingly, while general autophagy and pexophagy remain almost completely blocked during aging of the mutant, mitophagy flux does slightly increase identifying a PaATG24-independent form of mitophagy in *P. anserina*. This type of mitophagy appears to be less effective in mitochondrial quality control as conventional mitophagy of the wild type and thus cannot prevent accelerated aging. Future studies need to address the question which components of the autophagy machinery are required for the observed degradation of the mitophagy reporter. Unfortunately, until now, in filamentous fungi cargo receptors for mitophagy have not been identified. Filamentous fungi do not possess homologs of the yeast mitophagy cargo receptor ATG32 which recruits mitochondria to the autophagosome. However, it may be possible that the observed vacuolar degradation of the mitochondrial marker protein does not require the formation of autophagosomes and may proceed via micromitophagy and mitochondria-derived vesicles (Lemasters, 2014).

Due to the pleiotropic phenotype of the *PaAtg24* deletion mutant, it is not easy to precisely define the contribution of the different affected pathways on the aging process. Previous studies in *S. cerevisiae* revealed that peroxisome function is important for chronological aging and ablation of peroxisomal proteins result in a decreased lifespan (Lefevre et al., 2013). However, since cultivation on medium with oleate as sole carbon source restores the growth defect of the *ΔPaAtg24* mutant, we

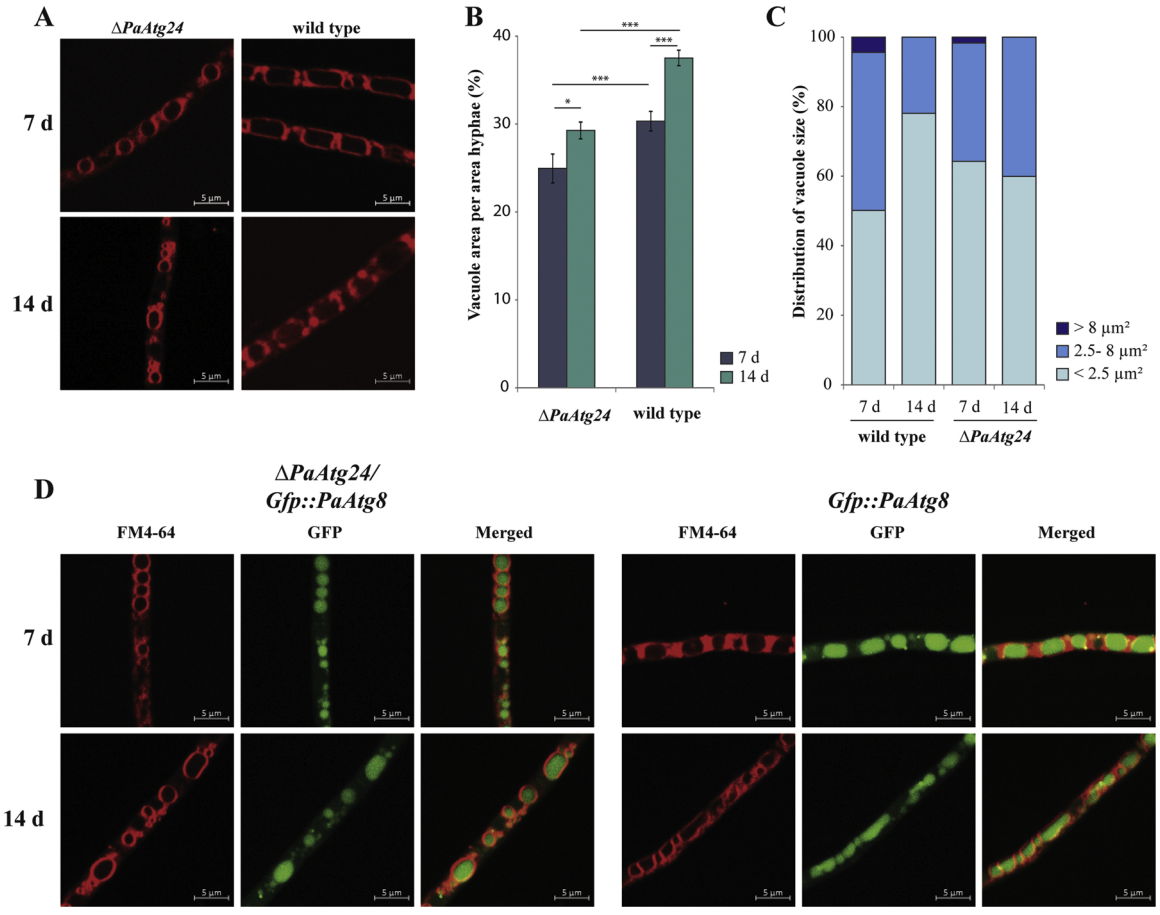

Fig. 4. Vacuole size and morphology depends on PaATG24.
(A–C) Staining of vacuolar membranes for 5 h with 2 µg/ml FM4–64 of 7- and 14-day-old *ΔPaAtg24* and wild-type strains. Cultivation was performed on M2 medium without nitrogen (M2-N) for one day before microscopic analysis for induction of vacuole formation. For analysis of vacuolar area per area hyphae and vacuolar size distribution, 7-day-old *ΔPaAtg24* (3650.1 µm² hyphae) and wild type (3630.2 µm² hyphae), as well as 2809.3 µm² wild-type hyphae and 2612.1 µm² hyphae of *ΔPaAtg24* in 14-day-old strains (n = 3, each) were analyzed. For distribution of vacuolar size, vacuoles were sorted in three categories: less than 2.5 µm², 2.5–8 µm² and more than 8 µm². (D) Fluorescence microscopy of 7- and 14-day-old *ΔPaAtg24/Gfp::PaAtg8* and *Gfp::PaAtg8* strains after cultivation for one day before microscopic analysis on M2-N medium. Staining of vacuole membrane was done with 2 µg/ml FM4–64 for 5 h.

assume that sufficient functional peroxisomes are present and peroxisome dysfunction does not explain the aging phenotype of the mutant. We rather suggest that a reduced mitophagy efficiency and impaired mitochondrial function profoundly contributes to the aging phenotype of *ΔPaAtg24*.

Since sorting nexins like ATG24/SNX4 are known to be involved in membrane dynamics, we investigated autophagosomes and vacuoles as major cellular compartments involved in autophagy. We found that, compared to the wild type, autophagosome abundance is increased in the mutant. Such an increase was also observed in a *TbAtg24* knockdown mutant of the human parasite *T. brucei* (Brennand et al., 2015). Moreover, in the *PaAtg24* deletion strain autophagosomes occur earlier during aging than in the wild type suggesting impairments in the efficient autophagic degradation of cellular components. The observed alterations in size and morphology of vacuoles, and the reduced coverage of the cell volume by vacuoles in *ΔPaAtg24* may lead to a reduced vacuolar degradation capacity. In the yeast *P. pastoris* it was reported that ablation of PpATG24 leads to an aberrant vacuole formation resulting in the inability to degrade peroxisomes due to an impaired fusion competence of vacuoles affecting macropexophagy or an impaired septation of the vacuolar compartment during micropexophagy (Ano et al., 2005). Impairments in autophagosome-vacuole fusion have been found to result from aberrant distribution of lipids. In a *ΔScSnx4/ΔScPsd1* strain of *S. cerevisiae* it was found that phosphatidylethanolamine-trafficking is impaired giving rise to an inability of autophagosome-vacuole fusion and to fragmentation of vacuoles (Ma et al., 2018). In contrast, in *P. anserina* the ablation of PaATG24 does not result in a stronger block of autophagosome-vacuole fusion. The accumulation of GFP in the mutant is comparable to that in the wild type. The reduction in autophagic flux in the mutant thus is rather due to a reduced size of vacuoles and a reduced coverage of the cell volume by vacuoles.

In yeast, a number of proteins have been shown to affect vacuolar size and shape. Among these, vacuolar protein sorting (VPS) proteins regulate the correct targeting of proteins to the vacuole (reviewed in: Aufschnaiter and Büttner, 2019). In *ΔPaAtg24* it is well possible that the altered size and morphology is a consequence of miss-sorting of vacuolar proteins and lipids which results in dysfunctional vacuoles. Several lines of evidence indicate a role of ATG24/SNX4 proteins in protein targeting and membrane trafficking. Human SNX4 interacts with components of the cytoskeleton and therefore is involved in vesicle trafficking, a miss-sorting of vesicles could lead to the ATG24-related impairments (Skånland et al., 2009; Traer et al., 2007). Further evidence comes from studies with *S. cerevisiae*, *S. pombe* and *F. graminearum*, where ATG24 is important for the endosomal sorting of the v-SNARE protein SNC1, which is involved in fusion of Golgi-derived secretory vesicles with the plasma membrane (Hettema et al., 2003; Lv et al., 2017; Zhao et al., 2016; Zheng et al., 2018). The observation that the ablation of FgATG24 in *F. graminearum* results in an impaired polarized growth, reduced pathogenicity and miss-sorting of FgSNC1 to

the vacuole (Zheng et al., 2018) and the demonstration that recycling of proteins from the vacuolar membrane to the endosome is coordinated by ATG24/SNX4 (Ma et al., 2017; Suzuki and Emr, 2018) support a role of this sorting nexin in the control of vacuolar function. It appears that the impairments in non-selective and selective autophagy in *ΔPaAtg24* may be the consequence of an altered membrane distribution or miss-sorting of proteins.

In yeast, as well as other fungi, it is known that ATG24 forms heterodimers with other sorting nexins like ATG20 or SNX41 (Nice et al., 2002; Zhao et al., 2016). These heterodimers fulfill distinct functions, depending on their interaction partner (Ma et al., 2017). In *S. cerevisiae*, the ATG24/SNX41 complex mediates retrograde sorting of ScATG27 (Ma et al., 2017), a protein implicated in selective autophagy. In *P. anserina* a homolog of SNX41 can be found (Uniprot B2AVK1), but no sequence homolog of ATG20. It may be possible that PaSNX41 is at least partially able to compensate the loss of PaATG24 explaining e.g. the residual mitophagy activity in the *PaAtg24* deletion mutant. However, data found in another filamentous fungus rather suggest non-overlapping functions of these two sorting nexins. In *M. oryzae* MoSNX41 has been shown to be important for pexophagy (Deng et al., 2013), while MoATG24/MoSNX4 is required for mitophagy (He et al., 2013) arguing against a functional redundancy.

Overall our findings highlight the importance of sorting nexins in the control of different cellular processes and link them to development and aging. The impact on different forms of autophagy complicates the conclusions to be drawn. In the work reported here a picture emerges indicating a special function of pexophagy in development and supports earlier findings about a role of mitophagy in aging (Knuppertz et al., 2017). In particular, this impact of mitophagy as part of a complex quality control network (Anand et al., 2013; Fischer et al., 2012) further emphasizes the importance of the effective control of a “healthy” population of mitochondria in aging and lifespan control.

Declaration of Competing Interest

The authors declare no conflict of interest.

Acknowledgements

This work was supported by grants of the German Research Foundation through SFB 1177 to HDO.

Appendix A. Supplementary data

Supplementary material related to this article can be found, in the online version, at doi:https://doi.org/10.1016/j.mad.2020.111211.

References

Ahola, S., Langer, T., MacVicar, T., 2019. Mitochondrial proteolysis and metabolic control. Cold Spring Harb. Perspect. Biol. 11. https://doi.org/10.1101/cshperspect.a033936.

Anand, R., Langer, T., Baker, M.J., 2013. Proteolytic control of mitochondrial function and morphogenesis. Biochim. Biophys. Acta 1833, 195–204. https://doi.org/10.1016/j.bbamcr.2012.06.025.

Ano, Y., Hattori, T., Oku, M., Mukaiyama, H., Baba, M., Ohsumi, Y., Kato, N., Sakai, Y., 2005. A sorting nexin PpAtg24 regulates vacuolar membrane dynamics during pexophagy via binding to phosphatidylinositol-3-phosphate. Mol. Biol. Cell 16, 446–457. https://doi.org/10.1091/mbc.e04-09-0842.

Aufschnaiter, A., Büttner, S., 2019. The vacuolar shapes of ageing: from function to morphology. Biochim. Biophys. Acta Mol. Cell. Res. 1866, 957–970. https://doi.org/10.1016/j.bbamcr.2019.02.011.

Bertrand, H., Griffiths, A.J., Court, D.A., Cheng, C.K., 1986. An extrachromosomal plasmid is the etiological precursor of kalDNA insertion sequences in the mitochondrial chromosome of senescent *Neurospora*. Cell 47, 829–837. https://doi.org/10.1016/0092-8674(86)90525-8.

Brennand, A., Rico, E., Rigden, D.J., Van Der Smissen, P., Courtoy, P.J., Michels, P.A., 2015. ATG24 represses autophagy and differentiation and is essential for homeostasy of the flagellar pocket in *Trypanosoma brucei*. PLoS One 10, e0130365. https://doi.org/10.1371/journal.pone.0130365.

Brust, D., Hamann, A., Osiewacz, H.D., 2010. Deletion of *PaAif2* and *PaAmid2*, two genes encoding mitochondrial AIF-like oxidoreductases of *Podospora anserina*, leads to increased stress tolerance and lifespan extension. Curr. Genet. 56, 225–235. https://doi.org/10.1007/s00294-010-0295-1.

Carman, P.J., Dominguez, R., 2018. BAR domain proteins-a linkage between cellular membranes, signaling pathways, and the actin cytoskeleton. Biophys. Rev. 10, 1587–1604. https://doi.org/10.1007/s12551-018-0467-7.

Chi, R.J., Harrison, M.S., Burd, C.G., 2015. Biogenesis of endosome-derived transport carriers. Cell. Mol. Life Sci. 72, 3441–3455. https://doi.org/10.1007/s00018-015-1935-x.

Cullen, P.J., 2008. Endosomal sorting and signalling: an emerging role for sorting nexins. Nat. Rev. Mol. Cell Biol. 9, 574–582. https://doi.org/10.1038/nrm2427.

Cummings, D.J., Belcour, L., Grandchamp, C., 1979. Mitochondrial DNA from *Podospora anserina*. II. Properties of mutant DNA and multimeric circular DNA from senescent cultures. Mol. Gen. Genet. 171, 239–250. https://doi.org/10.1007/bf00267578.

Daum, B., Walter, A., Horst, A., Osiewacz, H.D., Kühlbrandt, W., 2013. Age-dependent dissociation of ATP synthase dimers and loss of inner-membrane cristae in mitochondria. Proc. Natl. Acad. Sci. U. S. A. 110, 15301–15306. https://doi.org/10.1073/pnas.1305462110.

Deng, Y., Qu, Z., Naqvi, N.I., 2013. The role of Snx41-based pexophagy in *Magnaporthe* development. PLoS One 8, e79128. https://doi.org/10.1371/journal.pone.0079128.

Esser, K., 1997. In: In: King, R.C. (Ed.), Handbook of Genetics Vol 1. pp. 531–551 New York.

Fischer, F., Hamann, A., Osiewacz, H.D., 2012. Mitochondrial quality control: an integrated network of pathways. Trends Biochem. Sci. 37, 284–292. https://doi.org/10.1016/j.tibs.2012.02.004.

Gallon, M., Cullen, P.J., 2015. Retromer and sorting nexins in endosomal sorting. Biochem. Soc. Trans. 43, 33–47. https://doi.org/10.1042/BST20140290.

Haft, C.R., de la Luz Sierra, M., Barr, V.A., Haft, D.H., Taylor, S.I., 1998. Identification of a family of sorting nexin molecules and characterization of their association with receptors. Mol. Cell. Biol. 18, 7278–7287. https://doi.org/10.1128/mcb.18.12.7278.

Hamann, A., Krause, K., Werner, A., Osiewacz, H.D., 2005. A two-step protocol for efficient deletion of genes in the filamentous ascomycete *Podospora anserina*. Curr. Genet. 48, 270–275. https://doi.org/10.1007/s00294-005-0018-1.

He, Y., Deng, Y.Z., Naqvi, N.I., 2013. Atg24-assisted mitophagy in the foot cells is necessary for proper asexual differentiation in *Magnaporthe oryzae*. Autophagy 9, 1818–1827. https://doi.org/10.4161/auto.26057.

Hermanns, J., Asseburg, A., Osiewacz, H.D., 1994. Evidence for a life span-prolonging effect of a linear plasmid in a longevity mutant of *Podospora anserina*. Mol. Gen. Genet. 243, 297–307. https://doi.org/10.1007/bf00301065.

Hettema, E.H., Lewis, M.J., Black, M.W., Pelham, H.R., 2003. Retromer and the sorting nexins Snx4/41/42 mediate distinct retrieval pathways from yeast endosomes. EMBO J. 22, 548–557. https://doi.org/10.1093/emboj/cdg062.

Kadenbach, B., Munscher, C., Frank, V., Muller-Hocker, J., Napiwotzki, J., 1995. Human aging is associated with stochastic somatic mutations of mitochondrial DNA. Mutat. Res. 338, 161–172. https://doi.org/10.1016/0921-8734(95)00021-w.

Kikuma, T., Ohneda, M., Arioka, M., Kitamoto, K., 2006. Functional analysis of the ATG8 homologue Aoatg8 and role of autophagy in differentiation and germination in *Aspergillus oryzae*. Eukaryot. Cell 5, 1328–1336. https://doi.org/10.1128/EC.00024-06.

Knuppertz, L., Osiewacz, H.D., 2016. Orchestrating the network of molecular pathways affecting aging: role of nonselective autophagy and mitophagy. Mech. Ageing Dev. 153, 30–40. https://doi.org/10.1016/j.mad.2016.01.003.

Knuppertz, L., Osiewacz, H.D., 2017. Autophagy compensates impaired energy metabolism in CLPXP-deficient *Podospora anserina* strains and extends healthspan. Aging Cell 16, 704–715. https://doi.org/10.1111/acel.12600.

Knuppertz, L., Hamann, A., Pampaloni, F., Stelzer, E., Osiewacz, H.D., 2014. Identification of autophagy as a longevity-assurance mechanism in the aging model *Podospora anserina*. Autophagy 10, 822–834. https://doi.org/10.4161/auto.28148.

Knuppertz, L., Warnsmann, V., Hamann, A., Grimm, C., Osiewacz, H.D., 2017. Stress-dependent opposing roles for mitophagy in aging of the ascomycete *Podospora anserina*. Autophagy 1–16. https://doi.org/10.1080/15548627.2017.1303021.

Kramer, P., Jung, A.T., Hamann, A., Osiewacz, H.D., 2016. Cyclophilin D is involved in the regulation of autophagy and affects the lifespan of *P. anserina* in response to mitochondrial oxidative stress. Front. Genet. 7, 165. https://doi.org/10.3389/fgene.2016.00165.

Kroemer, G., Levine, B., 2008. Autophagic cell death: the story of a misnomer. Nat. Rev. Mol. Cell Biol. 9, 1004–1010. https://doi.org/10.1038/nrm2529.

Kück, U., Stahl, U., Esser, K., 1981. Plasmid-like DNA is part of mitochondrial DNA in *Podospora anserina*. Curr. Genet. 3, 151–156. https://doi.org/10.1007/BF00365719.

Kunstmann, B., Osiewacz, H.D., 2009. The S-adenosylmethionine dependent O-methyltransferase PaMTH1: a longevity assurance factor protecting *Podospora anserina* against oxidative stress. Aging (Albany NY) 1, 328–334. https://doi.org/10.18632/aging.100029.

Lecellier, G., Silar, P., 1994. Rapid methods for nucleic acids extraction from Petri dish-grown mycelia. Curr. Genet. 25, 122–123. https://doi.org/10.1007/bf00309536.

Lefevre, S.D., van Roermund, C.W., Wanders, R.J., Veenhuis, M., van der Klei, I.J., 2013. The significance of peroxisome function in chronological aging of *Saccharomyces cerevisiae*. Aging Cell 12, 784–793. https://doi.org/10.1111/acel.12113.

Lemasters, J.J., 2014. Variants of mitochondrial autophagy: types 1 and 2 mitophagy and micromitophagy (Type 3). Redox Biol. 2, 749–754. https://doi.org/10.1016/j.redox.2014.06.004.

Leprince, C., Le Scolan, E., Meunier, B., Fraisier, V., Brandon, N., De Gunzburg, J., Camonis, J., 2003. Sorting nexin 4 and amphiphysin 2, a new partnership between endocytosis and intracellular trafficking. J. Cell. Sci. 116, 1937–1948. https://doi.org/10.1242/jcs.00403.

Linnane, A.W., Marzuki, S., Ozawa, T., Tanaka, M., 1989. Mitochondrial DNA mutations

as an important contributor to ageing and degenerative diseases. Lancet 1, 642–645. https://doi.org/10.1016/s0140-6736(89)92145-4.
Linnane, A.W., Baumer, A., Maxwell, R.J., Preston, H., Zhang, C.F., Marzuki, S., 1990. Mitochondrial gene mutation: the ageing process and degenerative diseases. Biochem. Int. 22, 1067–1076.
Luce, K., Osiewacz, H.D., 2009. Increasing organismal healthspan by enhancing mitochondrial protein quality control. Nat. Cell Biol. 11, 852–858. https://doi.org/10.1038/ncb1893.
Lv, W., Wang, C., Yang, N., Que, Y., Talbot, N.J., Wang, Z., 2017. Genome-wide functional analysis reveals that autophagy is necessary for growth, sporulation, deoxynivalenol production and virulence in *Fusarium graminearum*. Sci. Rep. 7, 11062. https://doi.org/10.1038/s41598-017-11640-z.
Ma, M., Burd, C.G., Chi, R.J., 2017. Distinct complexes of yeast Snx4 family SNX-BARs mediate retrograde trafficking of Snc1 and Atg27. Traffic 18, 134–144. https://doi.org/10.1111/tra.12462.
Ma, M., Kumar, S., Purushothaman, L., Babst, M., Ungermann, C., Chi, R.J., Burd, C.G., 2018. Lipid trafficking by yeast Snx4 family SNX-BAR proteins promotes autophagy and vacuole membrane fusion. Mol. Biol. Cell 29, 2190–2200. https://doi.org/10.1091/mbc.E17-12-0743.
Melov, S., Lithgow, G.J., Fischer, D.R., Tedesco, P.M., Johnson, T.E., 1995. Increased frequency of deletions in the mitochondrial genome with age of *Caenorhabditis elegans*. Nucleic Acids Res. 23, 1419–1425. https://doi.org/10.1093/nar/23.8.1419.
Merry, T.L., Ristow, M., 2016. Mitohormesis in exercise training. Free Radic. Biol. Med. 98, 123–130. https://doi.org/10.1016/j.freeradbiomed.2015.11.032.
Meyer, N., Zielke, S., Michaelis, J.B., Linder, B., Warnsmann, V., Rakel, S., Osiewacz, H.D., Fulda, S., Mittelbronn, M., Münch, C., Behrends, C., Kögel, D., 2018. AT 101 induces early mitochondrial dysfunction and HMOX1 (heme oxygenase 1) to trigger mitophagic cell death in glioma cells. Autophagy 14, 1693–1709. https://doi.org/10.1080/15548627.2018.1476812.
Nemec, A.A., Howell, L.A., Peterson, A.K., Murray, M.A., Tomko Jr., R.J., 2017. Autophagic clearance of proteasomes in yeast requires the conserved sorting nexin Snx4. J. Biol. Chem. 292, 21466–21480. https://doi.org/10.1074/jbc.M117.817999.
Nice, D.C., Sato, T.K., Stromhaug, P.E., Emr, S.D., Klionsky, D.J., 2002. Cooperative binding of the cytoplasm to vacuole targeting pathway proteins, Cvt13 and Cvt20, to phosphatidylinositol 3-phosphate at the pre-autophagosomal structure is required for selective autophagy. J. Biol. Chem. 277, 30198–30207. https://doi.org/10.1074/jbc.M204736200.
Osiewacz, H.D., 1994. A versatile shuttle cosmid vector for the efficient construction of genomic libraries and for the cloning of fungal genes. Curr. Genet. 26, 87–90. https://doi.org/10.1007/bf00326309.
Osiewacz, H.D., 1996. Genetic analysis of senescence in *Podospora anserina*. In: Bos, C.J. (Ed.), Fungal Genetics. Marcel Dekker, New York, pp. 317–335.
Osiewacz, H.D., Esser, K., 1984. The mitochondrial plasmid of *Podospora anserina*: a mobile intron of a mitochondrial gene. Curr. Genet. 8, 299–305. https://doi.org/10.1007/BF00419728.
Osiewacz, H.D., Hermanns, J., Marcou, D., Triffi, M., Esser, K., 1989. Mitochondrial DNA rearrangements are correlated with a delayed amplification of the mobile intron (plDNA) in a long-lived mutant of *Podospora anserina*. Mutat. Res. 219, 9–15. https://doi.org/10.1016/0921-8734(89)90036-2.
Osiewacz, H.D., Skaletz, A., Esser, K., 1991. Integrative transformation of the ascomycete *Podospora anserina*: identification of the mating-type locus on chromosome VII of electrophoretically separated chromosomes. Appl. Microbiol. Biotechnol. 35, 38–45. https://doi.org/10.1007/bf00180633.
Osiewacz, H.D., Hamann, A., Zintel, S., 2013. Assessing organismal aging in the filamentous fungus *Podospora anserina*. Methods Mol. Biol. 965, 439–462. https://doi.org/10.1007/978-1-62703-239-1_29.
Piko, L., Hougham, A.J., Bulpitt, K.J., 1988. Studies of sequence heterogeneity of mitochondrial DNA from rat and mouse tissues: evidence for an increased frequency of deletions/additions with aging. Mech. Ageing Dev. 43, 279–293. https://doi.org/10.1016/0047-6374(88)90037-1.
Pinan-Lucarré, B., Paoletti, M., Dementhon, K., Coulary-Salin, B., Clave, C., 2003. Autophagy is induced during cell death by incompatibility and is essential for differentiation in the filamentous fungus *Podospora anserina*. Mol. Microbiol. 47, 321–333. https://doi.org/10.1046/j.1365-2958.2003.03208.x.
Pinan-Lucarré, B., Balguerie, A., Clave, C., 2005. Accelerated cell death in *Podospora* autophagy mutants. Eukaryot. Cell 4, 1765–1774. https://doi.org/10.1128/EC.4.11.1765-1774.2005.
Ristow, M., Zarse, K., 2010. How increased oxidative stress promotes longevity and metabolic health: the concept of mitochondrial hormesis (mitohormesis). Exp. Gerontol. 45, 410–418. https://doi.org/10.1016/j.exger.2010.03.014.
Rizet, G., 1953. Impossibility of obtaining uninterrupted and unlimited multiplication of the ascomycete *Podospora anserina*. C. R. Hebd. Seances Acad. Sci. 237, 838–840.
Ruprich-Robert, G., Berteaux-Lecellier, V., Zickler, D., Panvier-Adoutte, A., Picard, M., 2002. Identification of six loci in which mutations partially restore peroxisome biogenesis and/or alleviate the metabolic defect of pex2 mutants in *Podospora*. Genetics 161, 1089–1099.
Scheckhuber, C.Q., Osiewacz, H.D., 2008. *Podospora anserina*: a model organism to study mechanisms of healthy ageing. Mol. Genet. Genomics 280, 365–374. https://doi.org/10.1007/s00438-008-0378-6.
Skånland, S.S., Wälchli, S., Brech, A., Sandvig, K., 2009. SNX4 in complex with clathrin and dynein: implications for endosome movement. PLoS One 4, e5935. https://doi.org/10.1371/journal.pone.0005935.
Stahl, U., Lemke, P.A., Tudzynski, P., Kück, U., Esser, K., 1978. Evidence for plasmid like DNA in a filamentous fungus, the ascomycete *Podospora anserina*. Mol. Gen. Genet. 162, 341–343. https://doi.org/10.1007/bf00268860.
Suzuki, S.W., Emr, S.D., 2018. Retrograde trafficking from the vacuole/lysosome membrane. Autophagy 14, 1654–1655. https://doi.org/10.1080/15548627.2018.1496719.
Takano-Rojas, H., Zickler, D., Peraza-Reyes, L., 2016. Peroxisome dynamics during development of the fungus *Podospora anserina*. Mycologia 108, 590–602. https://doi.org/10.3852/15-112.
Traer, C.J., Rutherford, A.C., Palmer, K.J., Wassmer, T., Oakley, J., Attar, N., Carlton, J.G., Kremerskothen, J., Stephens, D.J., Cullen, P.J., 2007. SNX4 coordinates endosomal sorting of TfnR with dynein-mediated transport into the endocytic recycling compartment. Nat. Cell Biol. 9, 1370–1380. https://doi.org/10.1038/ncb1656.
Warnsmann, V., Osiewacz, H.D., 2016. Curcumin treatment affects mitochondrial respiration, induces autophagy and increases lifespan of the fungal aging model *Podospora anserina*. Endocytobiosis Cell Res. 27, 20–26.
Warnsmann, V., Meyer, N., Hamann, A., Kögel, D., Osiewacz, H.D., 2018. A novel role of the mitochondrial permeability transition pore in (-)-gossypol-induced mitochondrial dysfunction. Mech. Ageing Dev. 170, 45–58. https://doi.org/10.1016/j.mad.2017.06.004.
Zhao, D., Liu, X.M., Yu, Z.Q., Sun, L.L., Xiong, X., Dong, M.Q., Du, L.L., 2016. Atg20- and Atg24-family proteins promote organelle autophagy in fission yeast. J. Cell. Sci. 129, 4289–4304. https://doi.org/10.1242/jcs.194373.
Zheng, W., Lin, Y., Fang, W., Zhao, X., Lou, Y., Wang, G., Zheng, H., Liang, Q., Abubakar, Y.S., Olsson, S., Zhou, J., Wang, Z., 2018. The endosomal recycling of FgSnc1 by FgSnx41-FgSnx4 heterodimer is essential for polarized growth and pathogenicity in *Fusarium graminearum*. New Phytol. 219, 654–671. https://doi.org/10.1111/nph.15178.